

COMPARATIVE ANALYSIS of SOLAR RADIATION CHARACTERISTICS by USING INSOLATION MODELS

Abstract

Solar energy keeps increasing its potential to replace conventional sources of energy. However, the need for initial investment requires careful planning and efficient use of financial resources. The most vital part of such in-depth analysis is dependable data. Solar radiation values are of great significance to be able to estimate the potential of solar systems. On the other hand, solar radiation measurements are very limited in global scale. Thus, many models have been proposed in the literature to satisfy the need for the missing data. However, these models are dependent on the specifics of the region to be examined. Climatic conditions play significant role in model development. There are four climatic regions in Turkey and each of them need to be studied on its own. In this study, in order to design PV system for maximum efficiency under certain climatic conditions in Turkey, a comparative analysis of solar energy potential for two cities in the third climatic region is conducted.

Keywords: Photovoltaic Systems, Solar Energy, Panel Efficiency, Renewable Energy, Data Analysis.

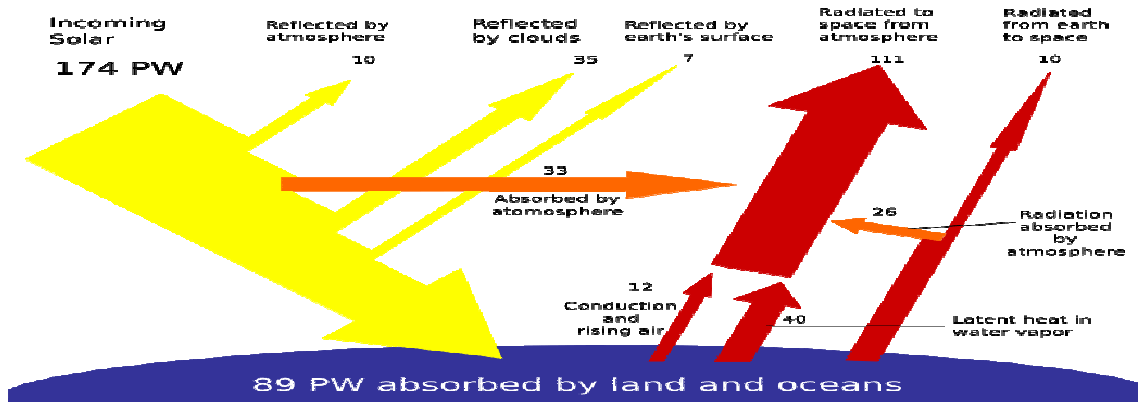
1. Introduction

Adoption of solar energy is vital to meet the growing energy demand worldwide. The fact that share of carbon-based fuels in energy supply need to be reduced due to the environmental concerns, intensify the research efforts on solar energy as one of the most significant alternative. Its ability to reduce environmental side-effects and relatively simple technology help increase the popularity among other sources of renewable energy. Fig.1 displays the renewable energy distribution of the world [1].



Fig. 1. Renewable energy distribution in the world [1]

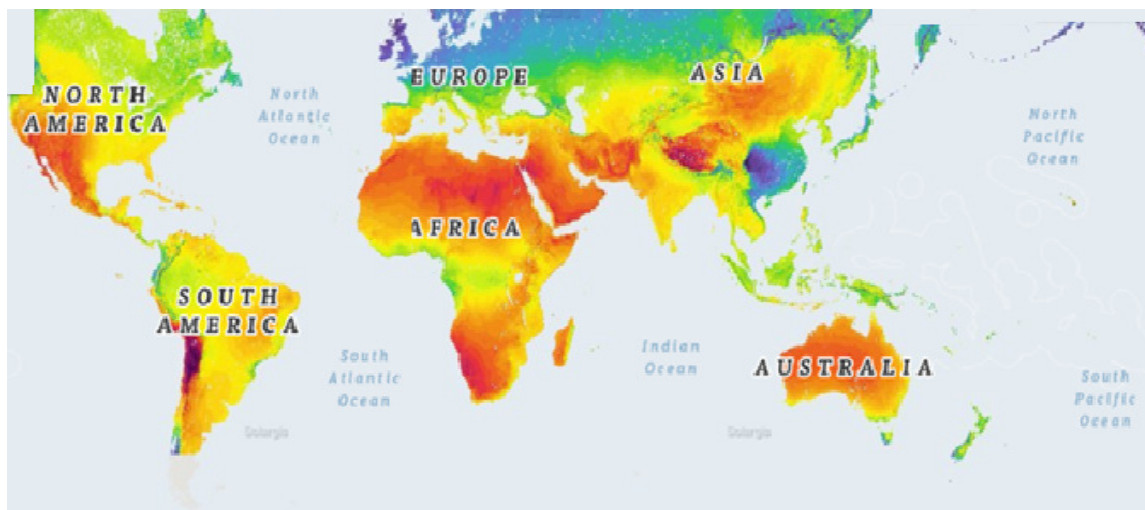
Fig. 2 shows solar radiation received on the earth. (A blackbody curve at the temperature of 5800 K is over plotted on the solar irradiance curve). In this figure, P_w is 10 15 Watts (PetaWatt) [2]. Global net radiation map is displayed in Fig. 3 [3].



30
31
32
33

Fig. 2. Solar Radiation received on the earth [2].

34 Measuring solar radiation which shows the energy radiated from the sun is a significant indicator of
 35 true potential of solar energy. Lack of meteorological stations raises the need for estimation models to
 36 assess the feasibility of solar energy investments. There is a wide range of deterministic models that
 37 have been developed for this purpose. In order to evaluate and compare the appropriateness of
 38 selected provinces in second climatic region for solar investments, a selection of these models are
 39 utilized in this study as discussed in the following section.
 40



41
42
43
44

Fig. 3. Global net solar radiation map [3]

45 In recent years, researchers have begun to focus on the evolution for local solar radiation related to
 46 model at photovoltaic system design. Many articles also pointed out that artificial neural network
 47 methodology is better than empiric models [4-6]. For four stations, Li et al. assessed eight sunshine
 48 duration fraction models in China. For calibration, data for eleven years are used. Four years of data
 49 are used for validation. The root mean square error (RMSE) is used as statistical indicator. RMSE of
 50 linear model changed from 1.26 to 0.72 MJ/m²day. RMSE of the eight models changed from 1.33 to
 51 0.7 MJ/m²day [7]. Tang et al. studied a hybrid model fixed by Koike and Yang for the prediction of
 52 daily solar radiation [8]. The model computed the clear sky index and clear-sky global radiation.
 53 These models used sunshine duration, thickness of ozone layer, air temperature, surface elevation,
 54 relative humidity, air pressure, and Angstrom turbidity as input parameters. For ninety-seven

55 meteorological stations in China, the obtained irradiation data from 2000 to 1993 used to confirm the
56 hybrid model. The root mean square error determined 0.7 and 1.3 MJ/m²day, respectively [9]. To
57 predict average hourly sun irradiation, Janjai et al. obtained a satellite-based model. For hours, the
58 relative root mean square error during 15:00 and 9:00 varied from 10.7% to 7.5% [10]. For 17 cities in
59 Iran, Behrang et al. searched eleven models by applying particle swarm optimization technique [11].
60 For two sites in Iran, Jamshid et al. researched three sunshine duration fraction (SDF) models one
61 modified sunshine duration fraction model. They used the method of support vector regression.
62 RMSE of them ranged between 2.14 and 3.70 MJ/m²day. The minimum and maximum temperature,
63 relative humidity, and sunshine duration selected as inputs for kernel function [12]. For Spain, Gorka
64 et al. compared three temperature-based empirical models, artificial neural networks (ANN), gene
65 expression programming, and adaptive neuro-fuzzy inference system. 2855 observations obtained
66 from 4 stations were utilized for testing and 4420 observations were utilized for training purposes.
67 The models used five combinations of minimum and maximum air temperature, clear sky radiation,
68 extraterrestrial radiation, and day number as inputs. The optimized GEP's RMSE varied between 3.31
69 and 3.49 MJ/m²day. The corresponding optimized adaptive neuro-fuzzy inference system's RMSE
70 changed between 3.33 and 3.14 MJ/m²day. The optimized artificial neural networks' root mean square
71 error of the applying other 3 combinations as inputs varied between 2.97 and 2.93 MJ/m²day [13]. For
72 79 sites in China with data for 10 years, Li et al. [14] applied a combined model (sine and cosine
73 functions). The mean absolute percentage error varied from 15.43% to 4.00% while RMSE changed
74 between 1.03 and 1.83 MJ/m²day. Amit et al. searched numerous articles that used ANN for the
75 estimation of sun irradiation in three reviews and predict sun irradiation on horizontal surfaces. They
76 pointed out that artificial neural network models were better than empiric models [15]. For 35 sites in
77 China Zang et al. [16] researched the same model by reducing two coefficients [17]. The mean
78 absolute percentage error and RMSE for the 35 sites ranged from 16.22%, to 4.33% and from 1.88 to
79 1.10 MJ/m²day, respectively. For seven sites in Spain, Almorox et al. researched eight non-sunshine
80 duration models which were primary based on the minimum and maximum temperature. In some
81 models, the characteristics of latitude, altitude, mean temperature, and the day of the year were
82 involved. The eight models' root mean square error changed from 3.25 to 2.70 MJ/m²day and the
83 mean absolute percentage error varied between 29.18% and 16.37% [18]. For sixty nine sites in
84 China, Zhou et al. analyzed six SDF models and used three SDF models to predict monthly average
85 sun irradiation. The altitude and latitude are added as parameters in modified models. The coefficient
86 values are derived separately. The sunshine duration fraction ranged from 1.634 to 1.636 MJ/m²day
87 [19]. For 3 sites in Liaoning City, China, Chen et al. researched 5 sunshine duration fraction models.
88 From each site, data for 35 years was obtained and 70% of the data were analyzed to derive empirical
89 coefficient values. For testing, 30% of the data were used. For each station, the empirical coefficient
90 values are determined. For Chaoyang, RMSE varied between 1.98 and 2.73 MJ/m²day, respectively
91 [20]. For four sites in Tunisia, Chelbi et al. researched five empiric models [21]. For six provinces in
92 Iran, Khorasanizadeh et al. assessed three mean SDF models and three NSDF models for the
93 prediction of average monthly global sun irradiation. In mean sunshine duration fraction models, the
94 relative humidity and temperature are added as parameters. Compared with sunshine duration fraction
95 models, the root mean square error of all models changed from 0.82 to 0.47MJ/m²day [22]. Wan Nik
96 et al. analyzed 6 mathematical expressions of the hourly solar radiation's ratio to daily radiation. For
97 monthly average hourly irradiation, the prediction was made. From three sites of Malaysia, data for
98 three years were utilized to test the models. They obtained that the relative root mean square error
99 varied from 26.49% to 8.22% [23]. For seven locations in Turkey, Hacer et al. investigated five
100 sunshine duration fraction models to predict monthly average radiation [24]. For 9 sites in China,
101 Zhao et al. researched the linear model. RMSE varied between 1.72 and 5.24 MJ/m²day [25]. For
102 Dezful, Iran, Behrang et al. investigated multi-layer perceptron network and radial basis function

103 network. Six combinations of the parameters (wind speed, relative humidity, day number,
104 evaporation, sunshine duration, and mean air temperature) were used. To train the models, 1398 days
105 were used. For testing, 214 days were used. The mean absolute percentage error changed from 5.21%
106 to 22.88%. [26]. For Shanghai in China, Yao et al. evaluated eighty nine monthly average radiation
107 models. Using various coefficients, many models are applied with same mathematical expressions.
108 For five sunshine duration fraction models in Shanghai, they derived new fitting coefficients [27]. For
109 4 sites in Thailand and 5 sites in Cambodian, Janjai et al. researched a satellite-based model. The root
110 mean square error is obtained as 1.13 MJ/m²day [28]. For twenty two sites in South Korea, Park et al.
111 searched linear empiric model [29]. El-Sebaï et al. performed three mean SDF models, three SDF
112 models and NSDF for the prediction of average monthly global sun irradiation for Saudi Arabia. The
113 characteristics grouped in mean sunshine duration fraction models were cloud cover, temperature, and
114 relative humidity. To derive novel empirical coefficient values, the data of nine years are employed.
115 RMSE of the 9 models ranged between 0.02 and 0.15 MJ/m²day [30, 31]. To predict hourly solar
116 irradiation, Shamim et al. used a fixed technique. To obtain the relative humidity and air pressure,
117 they used a meso-scale meteorological model for diverse atmospheric layers. By using available
118 measured data, they computed the cloud cover index with relative humidity and air pressure. By an
119 empirical correlation, they determined clear sky radiation and transmission factor to compute the
120 actual hourly solar irradiation. The clear sky radiation was predicted by applying irradiation transfer
121 model. For training, Data for one year was used. The root mean square error was obtained as 110.83
122 W/m² [32]. For four provinces in Turkey, Ahmet et al. researched cubic, linear, and quadratic empiric
123 models [33]. For two sites in Iran, Jamshid et al. researched two support vector regression models. As
124 inputs, the minimum and maximum temperature, sunshine duration, and relative humidity were used.
125 Root mean square errors were obtained from 1.63 to 4.47 MJ/m²day [34]. Bakirci investigated sixty
126 empiric models developed for the prediction of global monthly with average daily sun irradiation, in
127 which many of the predictions had same formulas just with diverse regressive constant parameters.
128 However, according to the conclusions of many articles, these constant parameters are generally based
129 on the investigation areas [35]. For 41 sites in China, Kevin et al. applied the linear Angstrom–Prescott
130 model to predict daily global sun irradiation. Those sites divided into seven sun climate regions and
131 nine thermal climate regions depending on diverse criteria, respectively. They applied the ANN model
132 using latitude, altitude, longitude, day number, sunshine duration fraction, and daily mean temperature
133 [36]. Kasra et al. presented four SDF models with data of nine years for Isfahan in Iran. Data of four
134 years were used to test the data. RMSE of them changed between 1.18 and 1.1 MJ/m²day [37]. For
135 Shiraz in Iran, Shahaboddin et al. assessed two SDF models, two mean SDF models and one non-
136 sunshine duration model. RMSE of the 5 models changed from 1.55 to 1.3 MJ/m²day [38]. In the
137 artificial neural networks model, Alvaro et al. applied the satellite data. The performance obtained is
138 reported to be very good [39]. Fariba et al. searched seventy eight empiric models. They grouped
139 them into four classes of models based on sun ray, cloud, meteorological characteristics, and
140 temperature. To develop a case study, they applied a few models from each of the classes for Iran.
141 The best performance is determined through a sun ray-based model with exponential expression [40].
142 For Turkey, Ozgoren et al. used the artificial neural networks model of multi non-linear regression to
143 obtain the best independent characteristics for input layer. They selected 10 characteristics (soil
144 temperature, month of the year, altitude, sunshine duration, cloudiness, minimum and maximum
145 atmospheric, mean atmospheric temperature, latitude, and wind speed). Levenberg-Marquardt
146 optimization algorithm was utilized to train the ANN [41]. For eleven meteorological sites on Tibetan,
147 Pan et al. investigated the exponential model based on temperature. The temperature difference is used
148 as input. To calibrate the model, data for 35 years were applied. For testing, data for 5 years were
149 applied. RMSE of the model changed from 2.54 to 3.24 MJ/m²day for all stations[42]. For twenty five
150 sites in Spain, Manzano et al. assessed the linear Angstrom–Prescott model. More than 10 years of

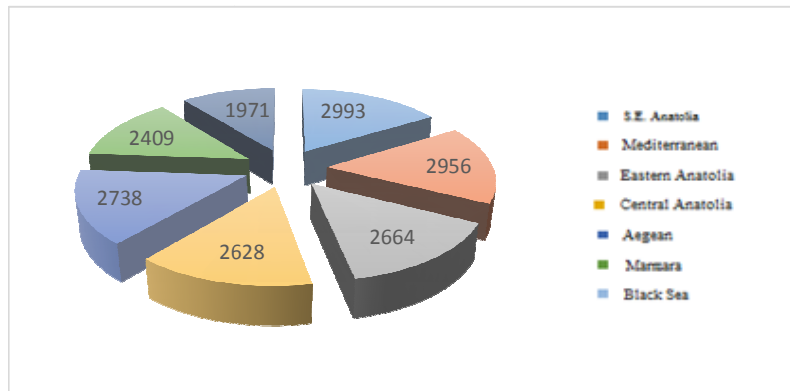
151 data was used for calibration purposes. Except for 4 sites, RMSE changed between 0.8 and 0.36
152 MJ/m²day [43]. Kadir studied seven different sunshine duration fraction models with data measured
153 from 18 sites in Turkey. Various models including exponential, logarithmic, quadratic, and linear
154 equations were used for the prediction of long-term average daily global solar radiation on monthly
155 basis. For the same sites, the performances of the applied models are obtained with slight differences
156 [44]. For Yazd in Iran, Fariba et al. analyzed the cloud-based model and Hargreaves model. The data
157 of sixteen years are utilized to obtain empiric constants. RMSE changed between 1.12 and 0.71
158 MJ/m²day [45]. For Gaize in Tibetan, Liu et al. investigated 3 non-sunshine duration models, 2 SDF
159 models and 3 modified SDF models. For calibration, 1085 days of data were analyzed while 701 days
160 of data were used to validation purposes. Root mean square error varied from 1.68 to 3.13 MJ/m²day.
161 For various seasons, they argued that deriving coefficient values respectively was unnecessary [46].
162 For 4 cities in India, Katiyar et al. searched the quadratic, cubic, and linear models for the prediction of
163 monthly average radiation using annual data. The values ranged from 0.8 to 0.43 MJ/m²day [47]. To
164 predict sun irradiation, Sun et al. assessed influence of autoregressive moving average model. They
165 investigated the data of 20 years from 2 sites in China [48]. In a year, Ayodele et al. performed a
166 function to present the clearness index's distribution. By using 7 years, the coefficient values
167 determined daily sun irradiation data. Except for October, the effectiveness of all months are obtained.
168 RMSE varied between 0.221 and 0.213 MJ/m²day [49]. For Iseyin in Nigeria, Lanre et al. used the
169 adaptive neuro-fuzzy inference system and ANN. Maximum and minimum temperature and sunshine
170 duration were used as inputs. Data of 6 years were obtained for model training while data of 15 years
171 were obtained to test the model. In testing and training phases, RMSE varied between 1.76 and 1.09
172 MJ/m²day, respectively [50]. Iranna et al. investigated sixteen non-sunshine duration models to
173 predict monthly average clearness values. As inputs, the moisture, wind speed, altitude, longitude,
174 relative humidity, and five other temperature related characteristics are used. Data for 875 sites are
175 evaluated to analyze the models [51]. To obtain the most effecting input characteristics for prediction,
176 Yadav et al. performed the Waikato Environment's software. They determined the minimum and
177 maximum temperature, average temperature, sunshine duration, and altitude as input characteristics,
178 while longitude and latitude were reported to be the least effective characteristics. The prediction was
179 for average monthly global sun irradiation. By the artificial neural networks, the maximum mean
180 absolute percentage error is obtained as 6.89% [52, 53]. Senkal proposed an artificial neural network
181 model using altitude, longitude, latitude, land surface temperature and two diverse surface emissivity
182 as inputs. The last 3 characteristics were determined using satellite data. To train the artificial neural
183 networks, one year of data from ten sites is used. The root mean square error in testing and training
184 stage were reported as 0.32 and 0.16 MJ/m²day, respectively [54]. For 4 provinces in Iran,
185 Khorasanizadeh et al. [55, 56] analyzed 6 models. The first model is based on exponential, the second
186 on polynomial and other four models on cosine and sine functions. These six models' RMSE varied
187 between 1.26 and 0.72 MJ/m²day, and the mean absolute percentage error changed from 5.72% to
188 3.38%. For Akure in Nigeria, Adaramola searched six non-sunshine duration models to predict long-
189 term monthly average sun irradiation and Angstrom-Page model. In non-sunshine duration models,
190 precipitation, relative humidity, and ambient temperature were used. RMSE changed between 8.25
191 and 4.78 MJ/m²day for the linear model [57]. For Bandar Abass province in Iran, Mohammadi et al.
192 [58] used support vector machine and wavelet transform algorithm. Data for 10 years were used to
193 train the models. The difference between minimum and maximum ambient temperatures, sunshine
194 duration fraction, water vapor pressure, relative humidity, extraterrestrial global sun irradiation, and
195 average ambient temperature are used as parameters. RMSE varied between 1.81 and 1.79 MJ/m²day,
196 respectively. Jiang et al. performed to priori association rules and Pearson correlation coefficients to
197 choose the relevant input characteristics. The wind speed, total average opaque sky cover,
198 precipitation, opaque sky cover, minimum and maximum temperature, average temperature, relative

199 humidity, daylight temperature, heating and cooling degree days were chosen as parameters [59]. Qin
 200 et al. used Levenberg-Marquardt algorithm with inputs including area temperature difference between
 201 night and daytime, air pressure rate number of days, vegetation index, mean area temperature, and
 202 monthly precipitation. For Tibetan Plateau, data of seven years from twenty two sites are used to train
 203 the artificial neural networks [60]. For Shiraz in Iran, Shahaboddin et al. used the artificial neural
 204 network and extreme learning machine algorithm. The relative humidity, average air temperature,
 205 temperature difference, and sunshine duration fraction are applied as inputs. 3 years of data were used
 206 for testing. RMSE varied between 0.93 and 0.86 MJ/m²day [61]. For twelve provinces in Turkey,
 207 Senkal et al. studied artificial neural networks model. The mean beam radiation, mean diffuse
 208 radiation, altitude, longitude, and latitude were utilized as inputs. The satellite-based method for the
 209 prediction of average monthly irradiation is proposed. Root mean square error changed from 2.75 and
 210 2.32 MJ/m²day [62]. For Saudi Arabia, Mohamed applied particle swarm optimization for training of
 211 the ANN. The longitude, altitude, latitude, sunshine duration, and month of the year were used as
 212 inputs. However, prediction was for monthly average global sun irradiation. To train the artificial
 213 neural networks, thirty one sites' data are utilized. The average mean absolute percentage error is
 214 obtained as 8.85% [63]. Antonio et al. designed a linear formula to correlate sun irradiation with the
 215 daily temperature variation and product of sunshine duration by using the power balance between
 216 adjacent atmosphere layer and soil layer [64].

217

218 **Climate, Solar Energy Potential and Electric Production in Usak and Tokat**

219 Equipment limitations and their high maintenance cost, have also limited the number of stations
 220 measuring solar radiation, thus meteorological variables are commonly being used in the calculation
 221 of solar radiation [65-67]. The land and sunshine period are of great significance for facilities to be
 222 established based on solar energy. Thus, comprehensive investigation need to be undertaken about
 223 climate, solar energy potential and current facilities. Among many models that have been developed
 224 to calculate amount of solar radiation, sunshine hours is the most widely utilized parameter [68].

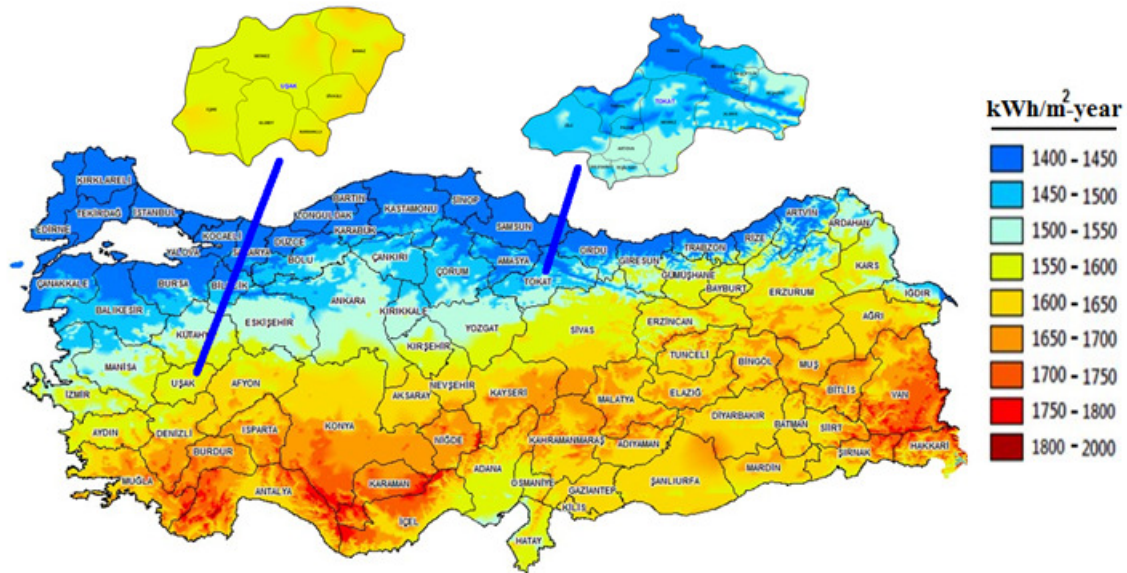


225

226

Fig. 4. Annual Total Solar Energy Period (hour-year)

227 As presented in Figure 4, more than half of Turkey possesses high potential of sunshine. Based on the
 228 study of General Directorate of Electrical Power Resources (EIE), average annual sunshine duration
 229 of Turkey is reported to be 2640 hours (7.2 hours/day) and average radiation intensity to be 1311
 230 kWh/m²-year (3.6 kWh/m²/day). Solar radiation maps for Usak and Tokat is displayed in Fig. 5.



231
232
233
234
235
236
237

Fig. 5. Solar radiation maps for Uşak and Tokat

In terms of solar energy potential, both cities are placed in the second region. Average solar radiation, radiation function frequency, radiation function phase shift, and latitude values for both cities are presented in Table 1.

Table 1. Radiation Values

City	Iort (MJ/m ² .day)	FGI (MJ/m ² .day)	FKI	Latitud e
Uşak	11.5	6.15	3.15	38.40
Tokat	12.5	7.76	6.19	40.00

238
239
240
241
242
243
244
245
246
247
248
249
250
251
252
253
254

In the next section, a comparative analysis is conducted on Matlab platform for both cities to reveal their solar radiation characteristics and potential.

2. Solar Radiation Intensity Calculation

Due to the climatic variations and geographic conditions, calculating amount of solar radiation depends on the specific region and requires the selection of the best model among others that are available in the literature. The model developed by Angstrom using radiation data and sunshine duration is the most commonly used one. Vartiainen et al. have proposed a statistical model to estimate the solar radiation amount through the use of data obtained from satellite [69]. Menges et al. provided a statistical comparison of daily total solar radiation on a horizontal surface in a specific city of Turkey with 50 different models in the literature [70]. Katiyar and Pandev have used solar radiation data from five different regions of India between 2001 and 2005 [71]. Consequently, they have developed Angstrom-type first, second, and third degree solar radiation models specific for each region. Monthly total radiation values of the developed model and measured values have also been compared.

2.1. Horizontal Surface

255 **2.1.1. Daily Total Solar Radiation**

256 Total solar radiation on horizontal surfaces on a given day can be calculated through the below
257 equation [72]:

$$258 \quad I = I_{ort} - FGI \cos \left[\frac{2\pi}{365} (n + FKI) \right] \quad 1$$

259 where

260 n: days,

261 FKI: radiation function phase shift,

262 FGI: radiation function frequency, and

263 I_{ort} : annual average of daily total radiation.

264

265 **2.1.2. Daily Diffuse Solar Radiation**

266 Total daily diffuse solar radiation on horizontal surfaces can be obtained using equation 2 [73].

$$267 \quad I_y = I(1-B)^2(1+3B^2) \quad 2$$

268 where,

269 I_o : Out-of-atmosphere radiation,

270 B: Transparency index.

271

272 **2.1.3. Momentary Total Solar Radiation**

273 Momentary total solar radiation on horizontal surfaces can be obtained using equation 2 [74, 75].

$$274 \quad I_o = \frac{24}{\pi} I_s (Cos(e) Cos(d) Sin(ws) + ws Sin(e) sin(d)) f \quad 3$$

275 where;

276 I_s (W/m^2): solar constant, e: latitude angle; w_s : sunrise hour angle f: solar constant correction factor,

277 d; declination angle can be calculated using the related tables and equations.

278 Out-of-atmosphere radiation can be calculated using equation 4 [73].

279

$$280 \quad I_{ts} = A_{ts} Cos \left[\frac{\pi}{t_{gi}} (t-12) \right] \quad 4$$

281

282 where;

283 A_{ts} : solar radiation and

284 t_{gi} : imaginary day length.

285

286 **2.1.4. Momentary Diffuse and Direct Solar Radiation**

287

288 Amount of momentary diffuse and direct solar radiation on horizontal surfaces can be obtained using

289 equations 5 and 6 [21, 22] where A_{ys} is function frequency.

$$290 \quad I_{ys} = A_{ys} C \cos \left[\frac{\pi}{t_g} (t-12) \right] \quad 5$$

$$291 \quad I_{ds} = I_{ts} = I_{ys} \quad 6$$

292 **2.2. Calculating Solar Radiation Intensity on Inclined Surface**

293 **2.2.1. Momentary Direct Solar Radiation**

294 Momentary direct solar radiation on inclined surfaces (30°-60°-90° angles) can be calculated using
295 the equation below [75].

$$296 \quad I_{be} = I_b R_b \quad 7$$

$$297 \quad R_b = \frac{\cos \theta}{\cos \theta_z} \quad 8$$

$$298 \quad \cos \theta_z = \sin d \sin e + \cos d \cos e \cos w \quad 9$$

$$299 \quad \cos \theta = \sin d \sin(e - \beta) + \cos d \cos(e - \beta) \cos w \quad 10$$

301

302 **2.2.2. Momentary Diffuse Solar Radiation**

303 Value of momentary diffuse radiation on inclined surfaces can be obtained using the equation
304 below [22].

$$305 \quad I_{ye} = R_y I_{ys} \quad 11$$

307 Conversion factor R_y for diffuse radiation can be calculated using equation below [75]:

308

$$309 \quad R_y = \frac{1 + \cos(a)}{2} \quad 12$$

311 R_y parameter provides the slope of the surface. For vertical surface ($a=90^\circ$), R_y value is 0.5. This
312 way, momentary values of diffuse radiation on inclined surfaces with 30°, 60°, 90° angles for 24-
313 hour time period can be calculated.

314

315 **2.2.3. Reflecting Momentary Solar Radiation**

316 Reflecting radiation on inclined surfaces [75] can be calculated using the equation below:

317

$$318 \quad I_{ya} = I_{ts} \rho \frac{1 + \cos(a)}{2} \quad 13$$

320 Environment reflection rate is shown with ρ parameter and used with average value of $\rho = 0.2$ in
321 calculations.

322

323 **2.2.4. Total Momentary Solar Radiation**

324 Momentary total radiation on inclined surfaces [75] can be obtained using equation below:

325

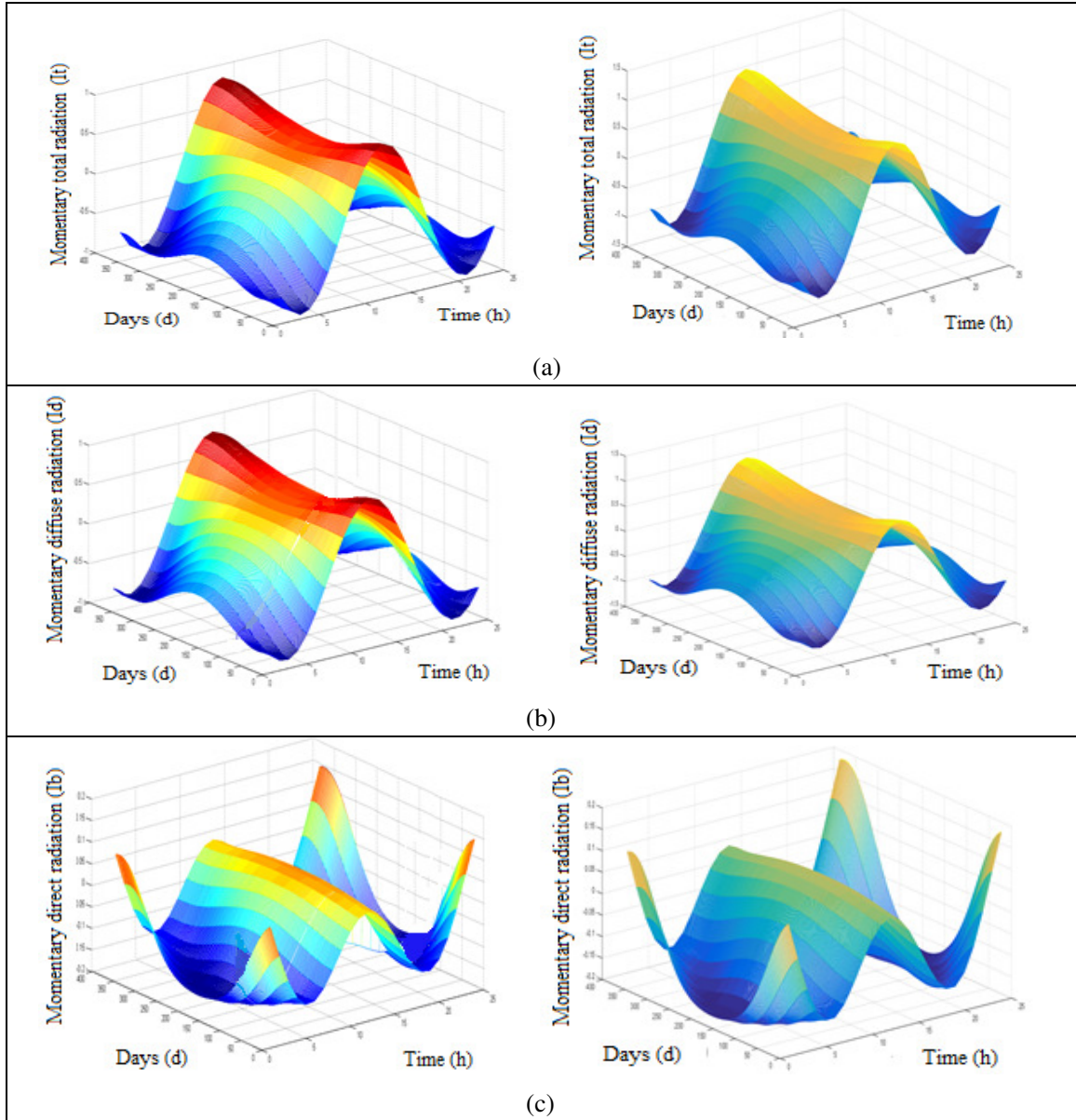
$$326 \quad I_t = I_{de} + I_{ye} + I_{ya} \quad 14$$

327

328 **3. Methodology**

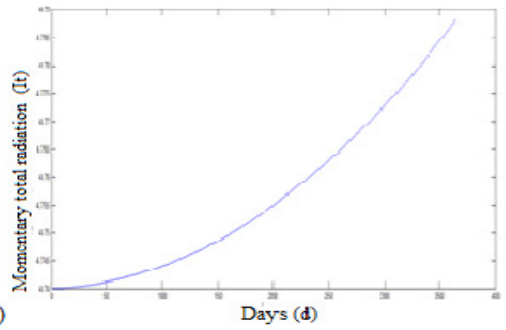
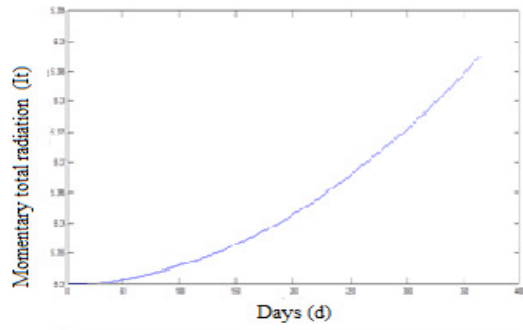
329 Figure 6 provides the values of; (a) change in annual momentary total solar radiation values for 24-
330 hour time period, (b) change in annual momentary diffuse solar radiation values per hour, (c) change

331 in annual momentary direct solar radiation values for 24-hour time period on horizontal surfaces.
 332 Figure 7 provides daily changes of; (a) total solar radiation values per day, (b) declination angle, (c)
 333 hourly angle for sunrise, (d) solar constant for correction factor, (e) solar radiation values out of
 334 atmosphere, (f) graph of function frequency (A_{ys}), (g) diffuse solar radiation (A_{ts}), (h) transparency
 335 index (B) for a horizontal surface.

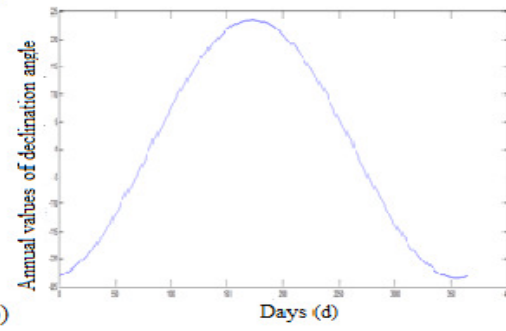
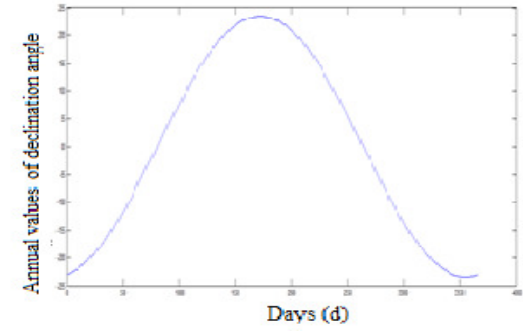


337

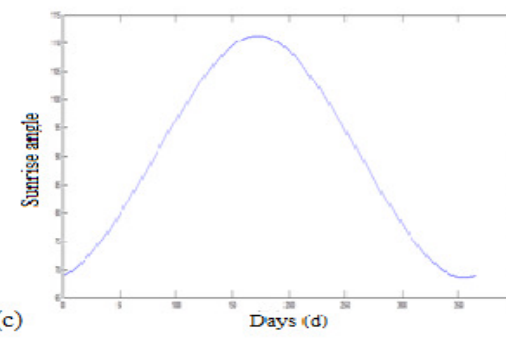
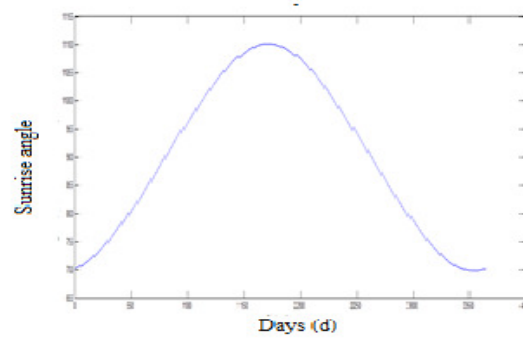
Fig. 6. Change of annual solar radiation values for 24-hour period on horizontal surfaces



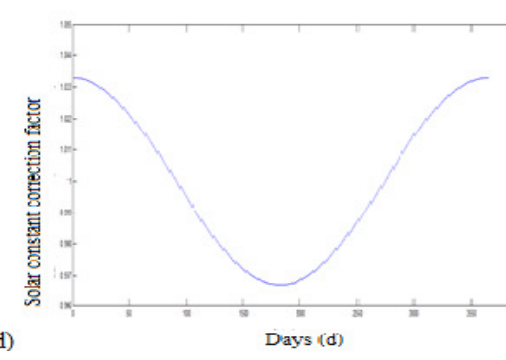
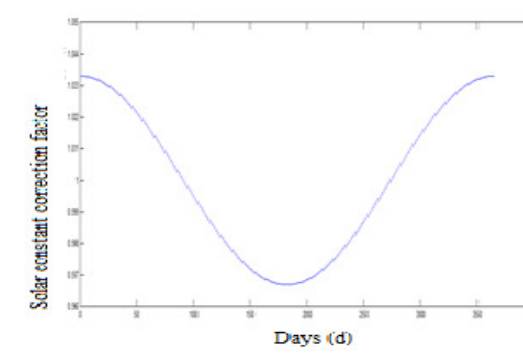
(a)



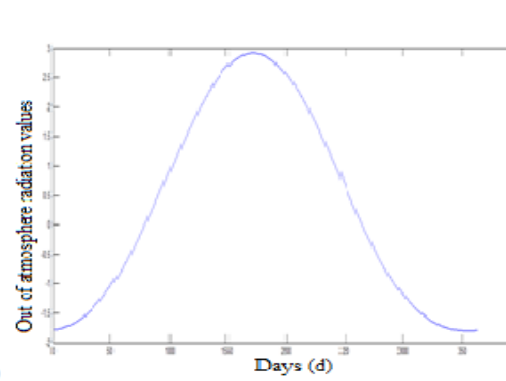
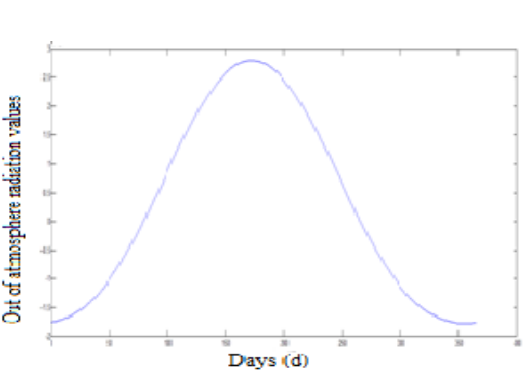
(b)



(c)



(d)



(e)

338
339

340

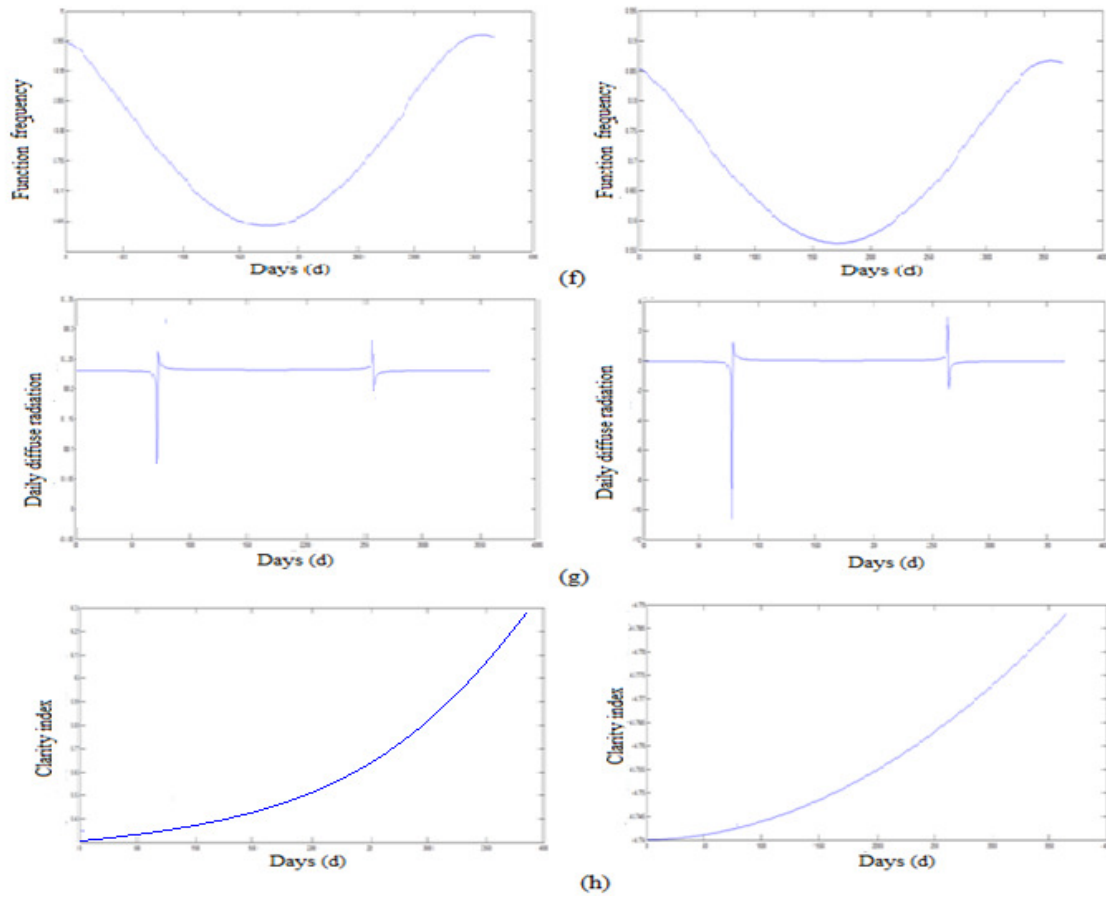
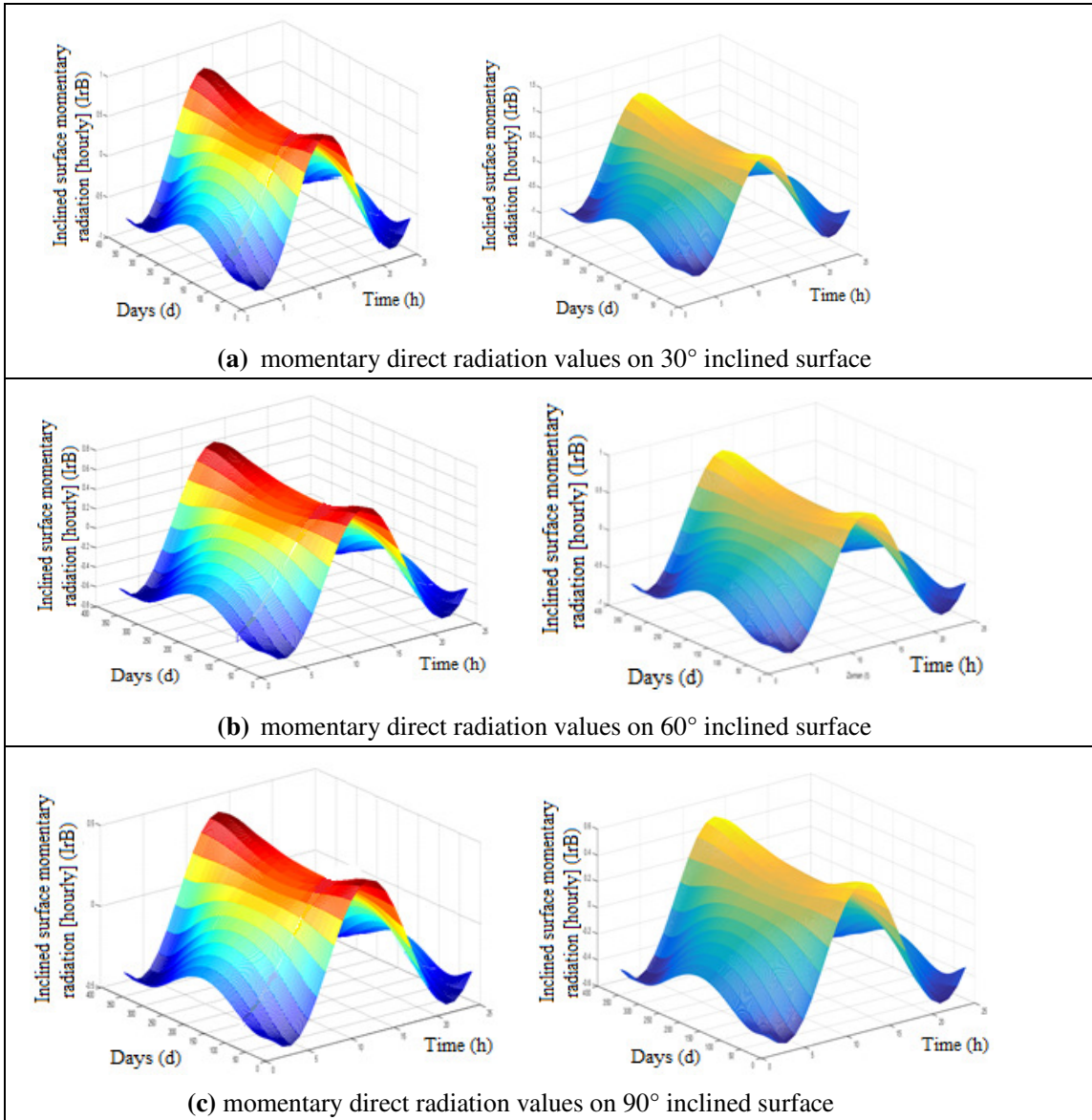


Fig. 7. Solar radiation on horizontal surfaces

Momentary direct radiation values with three different angles (30^0 , 60^0 and 90^0) for 24-hour time period are provided in Figure 8. The highest values for all three angles are obtained on the 355th day at 12:00, while the lowest values are obtained on the same day at 03:00.

341
 342
 343
 344
 345
 346
 347
 348
 349
 350
 351
 352
 353
 354
 355
 356



357
 358
 359
 360
 361
 362

Fig. 8. Annual momentary direct radiation values on inclined surface for 24-hour period

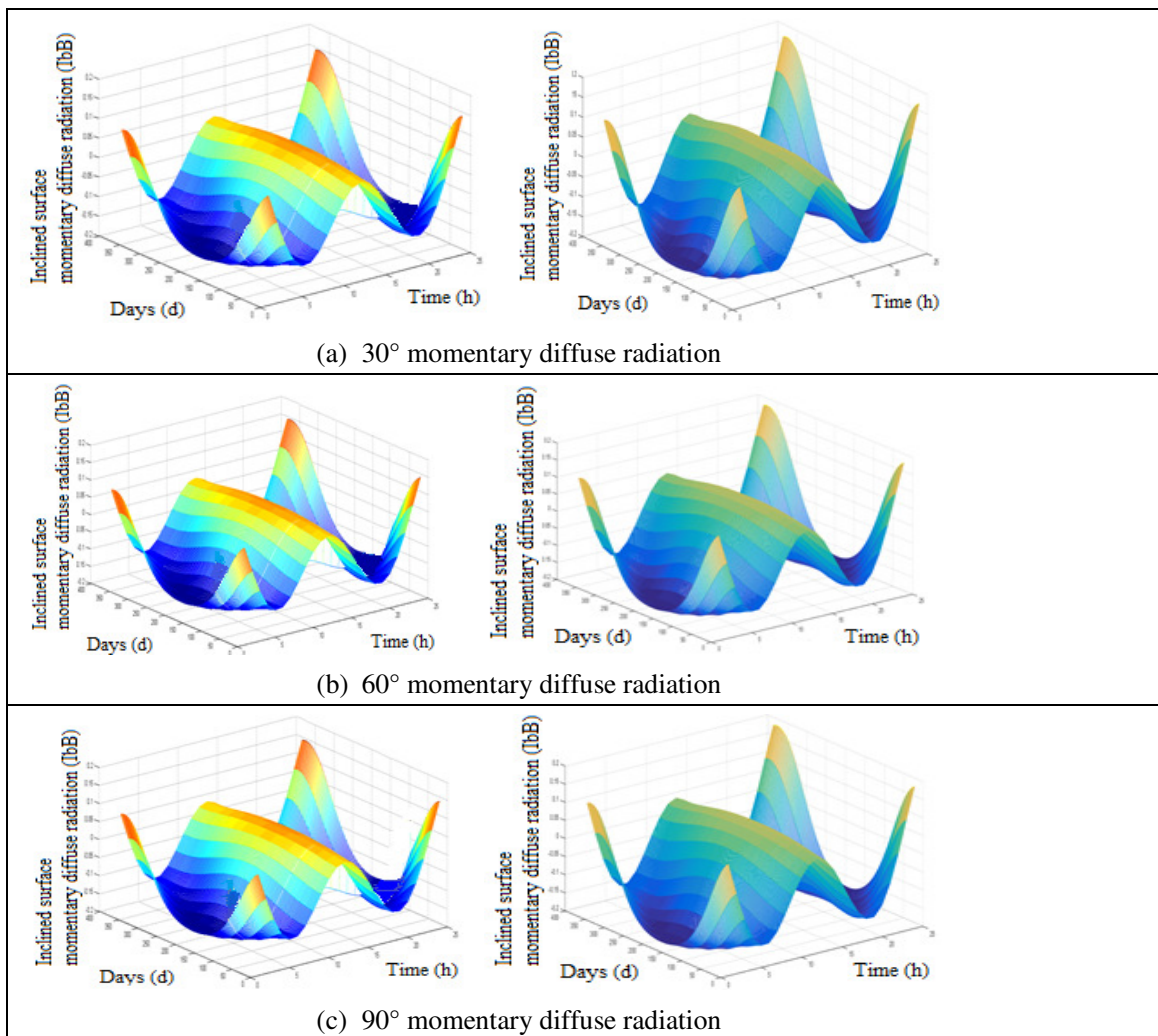


Fig. 9. Annual momentary diffuse radiation values for inclined surfaces

363
 364
 365
 366
 367
 368
 369
 370
 371
 372

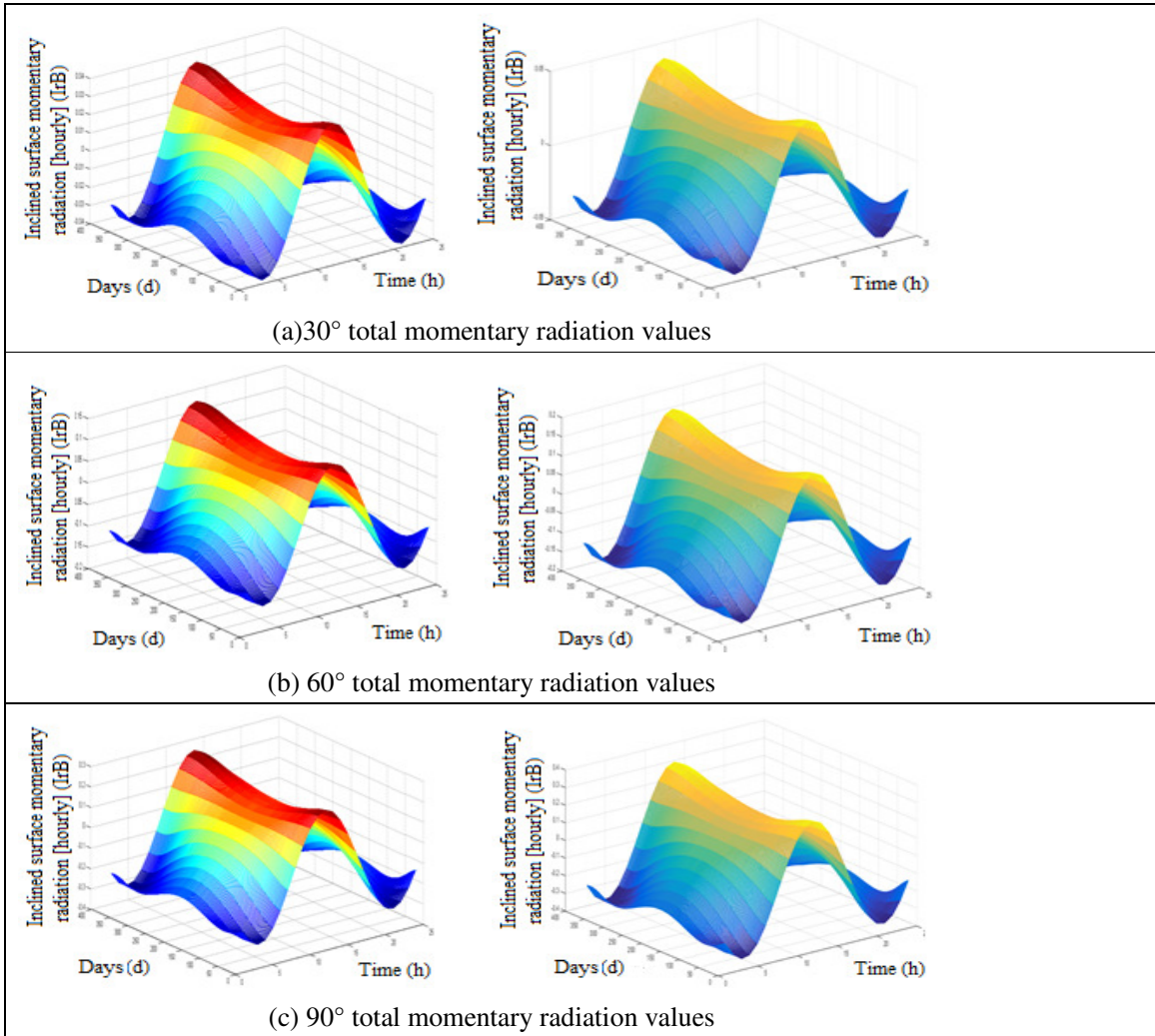


Fig. 10. Annual total momentary radiation values for inclined surface

373
 374
 375
 376
 377
 378
 379
 380
 381
 382
 383
 384
 385
 386
 387
 388

Annual momentary diffuse radiation values for three angles (30°, 60° and 90°) are provided in Figure 9. Annual values of total momentary solar radiation for 24-hour periods are provided in Figure 10.

389 **4. Findings and Results**

390 Based on the above analysis, true potential of both cities can be evaluated through the solar
 391 characteristics calculations provided in Table 2.

392

Table 2. Solar Radiation Attributes

Attributes		Usak	Tokat	Attributes		Usak	Tokat
Total radiation	Imax W/m2	5.3881	4.7858	Mom. dir. Rad.	I _{db} max(30°)	0.8678	0.8933
	I _{min} W/m2	5.3500	4.7400		I _{db} min(30°)	-	-
Declination angle	d _{max}	23.6798	23.4488		I _{db} max(60°)	0.6190	0.7807
	d _{min}	-23.7398	-23.4468		I _{db} min(60°)	-	-
Sunrise hour angle	w _{max}	112.1015	112.9271		I _{db} max(90°)	0.0397	0.4992
	w _{min}	70.9865	69.8123		I _{db} min(90°)	-	-
Out-of-Atmosphere Radiation	I _o (max) W/m2	281010	299215	Mom. Dif. rad.	I _b B _{max} (30°)	0.0395	0.1714
	I _o (min) W/m2	-177450	-189100		I _b B _{min} (30°)	-	-
Transp. Index	B _{max}	0.3330	0.3567		I _b B _{max} (60°)	0.0489	0.1898
	B _{min}	-0.0011	-0.0111		I _b B _{min} (60°)	-	-
Total diffuse radiation	I _y (max) W/m2	6.2822	4.7881		I _b B _{max} (90°)	0.0458	0.1911
	I _y (min) W/m2	5.1800	4.7400		I _b B _{min} (90°)	-	-
Function freq.	A _{ts} (max)	0.9500	0.8612				
	A _{ts} (min)	0.6418	0.5695				
Mom. Tot. Rad.	I _t (max)	1.7555	1.0011	Mom. reflecting rad.	I _r B _{max} (30°)	0.0378	0.0486
	I _t (min)	-0.9844	-1.1044		I _r B _{min} (30°)	-	-
Mom. Dif. Rad.	(A _{ys}) _{max}	0.8991	0.8112		I _r B _{max} (60°)	0.1191	0.1499
	(A _{ys}) _{min}	0.5799	0.5		I _r B _{min} (60°)	-	-
	I _d (max)	1.7853	0.9851		I _r B _{max} (90°)	0.2781	0.3001
	I _d (min)	-0.5865	-0.9956		I _r B _{min} (90°)	-	-
Mom. direct rad.	I _b (max)	0.0465	0.1854				
	I _b (min)	-0.1546	-0.1881				

393 Solar radiation values on inclined and horizontal surfaces are calculated through MATLAB software.
 394 Based on the calculations, the values of the indicators show that potential for photovoltaic systems in
 395 both cities correspond to expected levels. An integral of planning the photovoltaic systems is
 396 comparing the predicted values with the actual ones. The performance of the system depends on
 397 various parameters. Using realistic values of radiation has great importance for designing the
 398 optimum system. This study is aims to establish a reference for choosing the most efficient solar
 399 panel by relying on the real solar radiation values obtained for the most efficient photovoltaic system
 400 design. The solar radiation levels are evaluated to be at acceptable efficiency levels to design a
 401 photovoltaic system.

402

403 **References**

404 [1] <https://www.google.com.tr/search?q=solar+radiation+map>
 405 [2] http://en.wikipedia.org/wiki/File:Breakdown_of_the_incoming_solar_energy.svg
 406 [3] www.ren21.net

- 407 [4] Qazi A, Fayaz H, Wadi A, Raj RG, Rahim NA, Khan WA. The artificial neural network for solar
408 radiation prediction and designing solar systems: a systematic literature review. *J Clean Prod* 2015;
409 104:1–12.
- 410 [5] Piri J, Kisi O. Modelling solar radiation reached to the Earth using ANFIS, NNARX, and
411 empirical models (Case studies: Zahedan and Bojnurd stations). *J Atmos Sol Terr Phys* 2015; 123:39–
412 47.
- 413 [6] Teke A, Yıldırım HB, Çelik Ö. Evaluation and performance comparison of different models for
414 the estimation of solar radiation. *Renew Sustain Energy Rev* 2015; 50:1097–107
- 415 [7] Li H, Ma W, Lian Y, Wang X, Zhao L. Global solar radiation estimation with sunshine duration in
416 Tibet, China. *Renew Energy* 2011;36:3141–5.
- 417 [8] Yang K, Koike T, Ye B. Improving estimation of hourly, daily, and monthly solar radiation by
418 importing global data sets. *Agric Meteor* 2006; 137:43–55.
- 419 [9] Tang W, Yang K, He J, Qin J. Quality control and estimation of global solar radiation in China.
420 *Sol Energy* 2010; 84:466–75.
- 421 [10] Janjai S, Pankaew P, Laksanaboonsong J. A model for calculating hourly global solar radiation
422 from satellite data in the tropics. *Appl Energy* 2009; 86:1450–7.
- 423 [11] Behrang MA, Assareh E, Noghrehabadi AR, Ghanbarzadeh A. New sunshine-based models for
424 predicting global solar radiation using PSO (particle swarm optimization) technique. *Energy*
425 2011;36:3036–49.
- 426 [12] Piri J, Shamshirband S, Petković D, Tong CW, Rehman MHu. prediction of the solar radiation on
427 the earth using support vector regression technique. *Infrared Phys Technol* 2015; 68:179–85.
- 428 [13] Lam JC, Wan KKW, Yang L. Solar radiation modelling using ANNs for different climates in
429 China. *Energy Convers Manag* 2008; 49:1080–90.
- 430 [14] Li H, Ma W, Lian Y, Wang X. Estimating daily global solar radiation by day of year in China.
431 *Appl Energy* 2010; 87:3011–7.
- 432 [15] Yadav AK, Chandel SS. Solar radiation prediction using Artificial Neural Network techniques: a
433 review. *Renew Sustain Energy Rev* 2014; 33:772–81.
- 434 [16] Zang H, Xu Q, Bian H. Generation of typical solar radiation data for different climates of China.
435 *Energy* 2012; 38:236–48.
- 436 [17] Li H, Ma W, Lian Y, Wang X. Estimating daily global solar radiation by day of year in China.
437 *Appl Energy* 2010; 87:3011–7.
- 438 [18] Almorox J, Hontoria C, Benito M. Models for obtaining daily global solar radiation with
439 measured air temperature data in Madrid (Spain). *Appl Energy* 2011; 88:1703–9.
- 440 [19] Jin Z, Yezheng W, Gang Y. General formula for estimation of monthly average daily global solar
441 radiation in China. *Energy Convers Manag* 2005;46:257–68. [20] 55
- 442 [21] Chelbi M, Gagnon Y, Waewsak J. Solar radiation mapping using sunshine duration based models
443 and interpolation techniques: application to Tunisia. *Energy Convers Manag* 2015;101:203–15.
- 444 [22] Khorasanizadeh H, Mohammadi K. Introducing the best model for predicting the monthly mean
445 global solar radiation over six major cities of Iran. *Energy* 2013;51:257–66.
- 446 [23] Wan Nik WB, Ibrahim MZ, Samo KB, Muzathik AM. Monthly mean hourly global solar
447 radiation estimation. *Sol Energy* 2012; 86:379–87.
- 448 [24] Duzen H, Aydin H. Sunshine-based estimation of global solar radiation on horizontal surface at
449 Lake Van region (Turkey). *Energy Convers Manag* 2012;58:35–46.
- 450 [25] Zhao N, Zeng X, Han S. Solar radiation estimation using sunshine hour and air pollution index in
451 China. *Energy Convers Manag* 2013; 76:846–51.
- 452 [26] Behrang MA, Assareh E, Ghanbarzadeh A, Noghrehabadi AR. The potential of different artificial
453 neural network (ANN) techniques in daily global solar radiation modeling based on meteorological
454 data. *Sol Energy* 2010; 84:1468–80. [27] Yao W, Li Z, Wang Y, Jiang F, Hu L. Evaluation of global
455 solar radiation models for Shanghai, China. *Energy Convers Manag* 2014;84:597–612.
- 456 [28] Janjai S, Pankaew P, Laksanaboonsong J, Kitichantaropas P. Estimation of solar radiation over
457 Cambodia from long-term satellite data. *Renew Energy* 2011; 36:1214–20.
- 458 [29] Park J-K, Das A, Park J-H. A new approach to estimate the spatial distribution of solar radiation
459 using topographic factor and sunshine duration in South Korea. *Energy Convers Man*. 2015;101:30-9.
- 460 [30] El-Sebaai AA, Al-Ghamdi AA, Al-Hazmi FS, Faidah AS. Estimation of global solar radiation on
461 horizontal surfaces in Jeddah, Saudi Arabia. *Energy Policy* 2009;37:3645–9.

- 462 [31] El-Sebaili AA, Al-Hazmi FS, Al-Ghamdi AA, Yaghmour SJ. Global, direct and diffuse solar
463 radiation on horizontal and tilted surfaces in Jeddah, Saudi Arabia. *Appl Energy* 2010;87:568–76.
- 464 [32] Shamim MA, Remesan R, Bray M, Han D. An improved technique for global solar, *Renewable*
465 *and Sustainable Energy Reviews* 70 (2017) 314–329
- 466 [33] Teke A, Yıldırım HB. Estimating the monthly Global solar radiation for Eastern Mediterranean
467 Region. *Energy Convers Manag* 2014;87:628–35.
- 468 [34] Fortin JG, Anctil F, Parent L-É, Bolinder MA. Comparison of empirical daily surface incoming
469 solar radiation models. *Agric Meteor* 2008; 148:1332–40.
- 470 [35] Bakirci K. Models of solar radiation with hours of bright sunshine: a review. *Renew. Sustain.*
471 *Energy Rev* 2009; 13:2580–8.
- 472 [36] Wan KKW, Tang HL, Yang L, Lam JC. An analysis of thermal and solar zone radiation models
473 using an Angstrom–Prescott equation and artificial neural networks. *Energy* 2008; 33:1115–27.
- 474 [37] Mohammadi K, Shamshirband S, Anisi MH, Alam KA, Petković D. Support vector regression
475 based prediction of global solar radiation on a horizontal surface. *Energy Convers Manag*
476 2015;91:433–41.
- 477 [38] Shamshirband S, Mohammadi K, Yee PL, Petković D, Mostafaeipour A. A comparative
478 evaluation for identifying the suitability of extreme learning machine to predict horizontal global solar
479 radiation. *Renew Sustain Energy Rev* 2015;52:1031–42
- 480 [39] Linares-Rodriguez A, Ruiz-Arias JA, Pozo-Vazquez D, Tovar-Pescador J. An artificial neural
481 network ensemble model for estimating global solar radiation from Meteosat satellite images. *Energy*
482 2013; 61:636–45.
- 483 [40] Besharat F, Dehghan AA, Faghieh AR. Empirical models for estimating global solar radiation: a
484 review and case study. *Renew Sustain Energy Rev* 2013; 21:798–821.
- 485 [41] Ozgoren M, Bilgili M, Sahin B. Estimation of global solar radiation using ANN over Turkey.
486 *Expert Syst Appl* 2012; 39:5043–51.
- 487 [42] Pan T, Wu S, Dai E, Liu Y. Estimating the daily global solar radiation spatial distribution from
488 diurnal temperature ranges over the Tibetan Plateau in China. *Appl Energy* 2013; 107:384–93.
- 489 [43] Manzano A, Martín ML, Valero F, Armenta C. A single method to estimate the daily global solar
490 radiation from monthly data. *Atmos Res* 2015;166:70–82.
- 491 [44] Bakirci K. Correlations for estimation of daily global solar radiation with hours of bright
492 sunshine in Turkey. *Energy* 2009;34:485–501.
- 493 [45] Besharat F, Dehghan AA, Faghieh AR. Empirical models for estimating global solar radiation: a
494 review and case study. *Renew Sustain Energy Rev* 2013;21:798–821.
- 495 [46] Liu J, Liu J, Linderholm HW, Chen D, Yu Q, Wu D, et al. Observation and calculation of the
496 solar radiation on the Tibetan Plateau. *Energy Convers Manag* 2012; 57:23–32.
- 497 [47] Katiyar AK, Pandey CK. Simple correlation for estimating the global solar radiation on
498 horizontal surfaces in India. *Energy* 2010;35:5043–8.
- 499 [48] Sun H, Yan D, Zhao N, Zhou J. Empirical investigation on modeling solar radiation series with
500 ARMA–GARCH models. *Energy Convers Manag* 2015; 92:385–95.
- 501 [49] Ayodele TR, Ogunjuyigbe ASO. Prediction of monthly average global solar radiation based on
502 statistical distribution of clearness index. *Energy* 2015; 90:1733–42.
- 503 [50] Olatomiwa L, Mekhilef S, Shamshirband S, Petković D. Adaptive neuro-fuzzy approach for solar
504 radiation prediction in Nigeria. *Renew Sustain Energy Rev* 2015; 51:1784–91
- 505 [51] Korachagaon I, Bapat VN. General formula for the estimation of Global solar radiation on earth's
506 surface around the globe. *Renew Energy* 2012;41:394–400.
- 507 [52] Yadav AK, Malik H, Chandel SS. Selection of most relevant input parameters using WEKA for
508 artificial neural network based solar radiation prediction models. *Renew Sustain Energy Rev* 2014;
509 31:509–19.
- 510 [53] Yadav AK, Malik H, Chandel SS. Application of rapid miner in ANN based prediction of solar
511 radiation for assessment of solar energy resource potential of 76 sites in Northwestern India. *Renew*
512 *Sustain Energy Rev* 2015; 52:1093–106.
- 513 [54] Şenkal O. Modeling of solar radiation using remote sensing and artificial neural network in
514 Turkey. *Energy* 2010; 35:4795–801.
- 515 [55] Khorasanizadeh H, Mohammadi K. Prediction of daily global solar radiation by day of the year
516 in four cities located in the sunny regions of Iran. *Energy Convers Manag* 2013; 76:385–92. [56] 50.

- 517 [57] Adaramola MS. Estimating global solar radiation using common meteorological data in Akure,
518 Nigeria. *Renew Energy* 2012;47:38–44.
- 519 [58] Park J-K, Das A, Park J-H. A new approach to estimate the spatial distribution of solar radiation
520 using topographic factor and sunshine duration in South Korea. *Energy Convers Man.* 2015;101:30–9.
- 521 [59] Jiang H, Dong Y, Wang J, Li Y. Intelligent optimization models based on hard-ridge penalty and
522 RBF for forecasting global solar radiation. *Energy Convers Manag* 2015; 95:42–58.
- 523 [60] Qin J, Chen Z, Yang K, Liang S, Tang W. Estimation of monthly-mean daily global solar
524 radiation based on MODIS and TRMM products. *Appl Energy* 2011; 88:2480–9.
- 525 [61] Shamshirband S, Mohammadi K, Yee PL, Petković D, Mostafaiepour A. A comparative
526 evaluation for identifying the suitability of extreme learning machine to predict horizontal global solar
527 radiation. *Renew Sustain Energy Rev* 2015; 52:1031–42.
- 528 [62] Şenkal O, Kuleli T. Estimation of solar radiation over Turkey using artificial neural network and
529 satellite data. *Appl Energy* 2009; 86:1222–8.
- 530 [63] Mohandes MA. Modeling global solar radiation using particle swarm optimization (PSO). *Sol*
531 *Energy* 2012; 86:3137–45. [64] 29
- 532 [65] Chen RS, Lu SH, Kang ES, et al. Estimating daily global radiation using two types of revised
533 models in China. *Energy Convers Manage* 2006;47:865–78.
- 534 [66] Yorukoglu M, Celik AN. A critical review on the estimation of daily global solar radiation from
535 sunshine duration. *Energy Convers Manage* 2006;47:2441–50.
- 536 [67] Almorox J, Hontoria C. Global radiation estimation using sunshine duration in Spain. *Energy*
537 *Convers Manage* 2004;45:1529–35.
- 538 [68] Lei Zhao, Xuhui Lee, Shoudong Liu, Correcting surface solar radiation of two data assimilation
539 systems against FLUXNET observations in North America *Journal of Geophysical Research:*
540 *Atmospheres*, Vol 118 (17), 2013
- 541 [69] Vartiainen, E., 2000. A new approach to estimating the diffuse irradiance on inclined surfaces.
542 *Renewable Energy*, 20: 45–64.
- 543 [70] Hakan Okyay Menges, Can Ertekin, Mehmet Hakan Sonmete, Evaluation of global solar
544 radiation models for Konya, Turkey, *Energy Conversion and Management*, Volume 47, Issues 18–19,
545 November 2006, Pages 3149-3173
- 546 [71] C. K. Pandey and A. K. Katiyar, *Solar Radiation: Models and Measurement Techniques*, *Journal*
547 *of Energy*, Vol. 2013 (2013)
- 548 [72] Derse MS. (2014) Batman'ın İklim Koşullarında Eğimli Düzleme Gelen Güneş Işınımının Farklı
549 Açı Değerlerinde Belirlenmesi Sayfa 37-47 Batman
- 550 [73] Miguel, A.D., Bilbao, J., Aguiar, R., Kambezidis, H., and Negro, E., 2001. Diffuse solar
551 irradiation model evaluation in the North mediterranean belt area. *Solar Energy*, 70: 143–153.
- 552 [74] Notton, G., Poggi, P., and Cristofari, C., (2006), Predicting hourly solar irradiations on inclined
553 surfaces based on the horizontal measurements: Performances of the association of well-known
554 mathematical models. *Energy Conversion and Management*, 47: 1816–1829.
- 555 [75] Erbs, DG, Klein, SA., Duffie, JA., (1982), Estimation of the diffuse radiation fraction for hourly,
556 daily and monthly-average global radiation, *Solar Energy*, 28(4): 293–302.